



HAL
open science

Bulk magnetic terahertz metamaterials based on dielectric microspheres

Michal Sindler, Christelle Kadlec, Filip Dominec, Petr Kužel, Catherine Elissalde, Ahmad Kassas, Julien Lesueur, Dominique Bernard, Patrick Mounaix, Hynec Němec

► **To cite this version:**

Michal Sindler, Christelle Kadlec, Filip Dominec, Petr Kužel, Catherine Elissalde, et al.. Bulk magnetic terahertz metamaterials based on dielectric microspheres. *Optics Express*, 2016, 24 (16), pp.18340-18345. 10.1364/OE.24.018340 . hal-01373166

HAL Id: hal-01373166

<https://hal.science/hal-01373166>

Submitted on 19 Jan 2021

HAL is a multi-disciplinary open access archive for the deposit and dissemination of scientific research documents, whether they are published or not. The documents may come from teaching and research institutions in France or abroad, or from public or private research centers.

L'archive ouverte pluridisciplinaire **HAL**, est destinée au dépôt et à la diffusion de documents scientifiques de niveau recherche, publiés ou non, émanant des établissements d'enseignement et de recherche français ou étrangers, des laboratoires publics ou privés.

Bulk magnetic terahertz metamaterials based on dielectric microspheres

M. ŠINDLER,^{1,2} C. KADLEC,¹ F. DOMINEC,¹ P. KUŽEL,¹
C. ELISSALDE,³ A. KASSAS,³ J. LESSEUR,³ D. BERNARD,³ P.
MOUNAIX,² AND H. NĚMEC^{1,*}

¹*Institute of Physics, Academy of Sciences of the Czech Republic, Na Slovance 1999/2, 182 21 Prague, Czech Republic*

²*Univ. Bordeaux, IMS UMR CNRS 5218, 351 cours de la Liberation, 33405 Talence, France*

³*ICMCB, Univ. Bordeaux, CNRS, UPR 9048, 33600 Pessac cedex, France*

**nemec@fzu.cz*

Abstract: Rigid metamaterials were prepared by embedding TiO₂ microspheres into polyethylene. These structures exhibit a series of Mie resonances where the lowest-frequency one is associated with a strong dispersion in the effective magnetic permeability. Using time-domain terahertz spectroscopy, we experimentally demonstrated the magnetic nature of the observed resonance. The presented approach shows a way for low-cost massive fabrication of mechanically stable terahertz metamaterials based on dielectric microresonators.

© 2016 Optical Society of America

OCIS codes: (160.3918) Metamaterials; (300.6495) Spectroscopy, terahertz.

References and links

1. D. R. Smith, J. B. Pendry, and M. C. K. Wiltshire, "Metamaterials and negative refractive index," *Science* **305**, 788 (2004).
2. J. B. Pendry, A. J. Holden, D. J. Robbins, and W. J. Stewart, "Magnetism from conductors and enhanced nonlinear phenomena," *IEEE Trans. Microwave Theory Tech.* **47**, 2075 (1999).
3. J. B. Pendry, "Negative refraction makes a perfect lens," *Phys. Rev. Lett.* **85**, 3966 (2000).
4. S. A. Ramakrishna, "Physics of negative refractive index materials," *Rep. Prog. Phys.* **68**, 449 (2005).
5. T. J. Yen, W. J. Padilla, N. Fang, D. C. Vier, D. R. Smith, J. B. Pendry, D. N. Basov, and X. Zhang, "Terahertz magnetic response from artificial materials," *Science* **303**, 1494 (2004).
6. H.-T. Chen, W. J. Padilla, J. M. O. Zide, A. C. Gossard, A. J. Taylor, and R. D. Averitt, "Active terahertz metamaterial devices," *Nature* **444**, 597 (2006).
7. H. Tao, A. C. Strikwerda, K. Fan, W. J. Padilla, X. Zhang, and R. D. Averitt, "Reconfigurable terahertz metamaterials," *Phys. Rev. Lett.* **103**, 147401 (2009).
8. S. O'Brien, and J. B. Pendry, "Photonic band-gap effects and magnetic activity in dielectric composites," *J. Phys.: Condens. Matter* **14**, 4035 (2002).
9. Q. Zhao, B. Du, L. Kang, H. Zhao, Q. Xie, B. Li, X. Zhang, J. Zhou, L. Li, and Y. Meng, "Tunable negative permeability in an isotropic dielectric composite," *Appl. Phys. Lett.* **92**, 051106 (2008).
10. A. A. Basharin, M. Kafesaki, E. N. Economou, C. M. Soukoulis, V. A. Fedotov, V. Savinov, and N. I. Zheludev, "Dielectric metamaterials with toroidal dipolar response," *Phys. Rev. X* **5**, 011036 (2015).
11. H. Němec, P. Kužel, F. Kadlec, C. Kadlec, R. Yahiaoui, and P. Mounaix, "Tunable terahertz metamaterials with negative permeability," *Phys. Rev. B* **79**, 241108(R) (2009).
12. R. A. Parker, "Static dielectric constant of rutile (TiO₂), 1.6-1060°K," *Phys. Rev.* **124**, 1719 (1961).
13. H. Němec, C. Kadlec, F. Kadlec, P. Kužel, R. Yahiaoui, U.-C. Chung, C. Elissalde, M. Maglione, and P. Mounaix, "Resonant magnetic response of TiO₂ microspheres at terahertz frequencies," *Appl. Phys. Lett.* **100**, 061117 (2012).
14. F. Dominec, C. Kadlec, H. Němec, P. Kužel, and F. Kadlec, "Transition between metamaterial and photonic-crystal behavior in arrays of dielectric rods," *Opt. Express* **22**, 30492 (2014).
15. A. F. Oskooi, D. Roundy, M. Ibanescu, P. Bermel, J. D. Joannopoulos, and S. G. Johnson, "Meep: A flexible free-software package for electromagnetic simulations by the FDTD method," *Comput. Phys. Commun.* **181**, 687 (2010).
16. A. M. Nicolson, and G. F. Ross, "Measurement of the intrinsic properties of materials by time-domain techniques," *IEEE Trans. Instrum. Meas.* **19**, 377 (1970).
17. W. Weir, "Automatic measurement of complex dielectric constant and permeability at microwave frequencies," *Proc. IEEE* **62**, 33 (1974).
18. D. R. Smith, S. Schultz, P. Markoš, and C. M. Soukoulis, "Determination of effective permittivity and permeability of metamaterials from reflection and transmission coefficients," *Phys. Rev. B* **65**, 195104 (2002).

19. Th. Koschny, P. Markoš, D.R. Smith, and C. M. Soukoulis, "Resonant and antiresonant frequency dependence of the effective parameters of metamaterials," *Phys. Rev. E* **68**, 065602 (2003).
20. V. M. Agranovich, Yu. N. Gartstein, "Spatial dispersion and negative refraction of light," *Phys. Usp.* **49**, 1029 (2006).
21. P. Kužel, H. Němec, F. Kadlec, and C. Kadlec, "Gouy shift correction for highly accurate refractive index retrieval in time-domain terahertz spectroscopy," *Opt. Exp.* **18**, 15338 (2010).
22. L. Duvillaret, F. Garet, and J.-L. Coutaz, "Highly precise determination of optical constants and sample thickness in terahertz time-domain spectroscopy," *Appl. Opt.* **38**, 409 (1999).
23. H. Němec, F. Kadlec, P. Kužel, L. Duvillaret, J.-L. Coutaz, "Independent determination of the complex refractive index and wave impedance by time-domain terahertz spectroscopy," *Opt. Commun.* **260**, 175 (2006).
24. V. Yannopapas, and A. Moroz, "Negative refractive index metamaterials from inherently non-magnetic materials for deep infrared to terahertz frequency ranges," *J. Phys.: Condens. Matter* **17**, 3717 (2005).
25. W. T. Doyle, "Optical properties of a suspension of metal spheres," *Phys. Rev. B* **39**, 9852 (1989).

1. Introduction

Electromagnetic metamaterials are artificial media with optical response strongly modified due to structuring on a macroscopic scale. A proper design allows on-demand tailoring of various unique effective optical properties not found in natural materials [1], like magnetic response above sub-terahertz frequencies [2]. The negative magnetic permeability is a prerequisite for achieving a negative refractive index, which can find a variety of applications including imaging beyond the diffraction limit [3,4].

Most metamaterials for the terahertz (THz) spectral range are nowadays based on metallic resonators which offer the possibility to design a large variety of functionalities [5–7]. Micrometer-sized resonant metallic structures are prepared by optical lithography techniques which require clean room facilities. All-dielectric metamaterials may be easier to fabricate while they still provide the possibility to achieve a tunable magnetic response e.g. close to the first Mie resonance [8–11].

In this paper, we focus on the investigation of THz metamaterials based on TiO₂ microsphere resonators. TiO₂ is a suitable dielectric material due to its high permittivity and low dielectric losses [12]. In our previous work, the TiO₂ microspheres were dispersed in air, forming nearly a single-layer sample enclosed between two sapphire wafers [13]. Here we embedded the TiO₂ microspheres into a polyethylene matrix which enabled us to prepare a rigid bulk metamaterial with a controllable concentration of microresonators. We performed measurements using time-domain THz spectroscopy to characterize fully the response of such structures and to confirm its magnetic character. The retrieved spectra of effective dielectric permittivity and magnetic permeability are discussed within Mie theory and Maxwell-Garnett effective medium model.

2. Sample

TiO₂ microspheres with a diameter of a few tens of micrometers were prepared by a bottom up approach. A liquid suspension of TiO₂ nanoparticles was first spray-dried producing fragile TiO₂ microspheres. These were subsequently sintered in a furnace at 1200°C for two hours, in order to consolidate individually each sphere (see Fig. 1). Using X-ray microtomography (Ultra of Zeiss-Xradia), we found that the particles show polycrystalline rutile structure with a porosity of 15%. The microspheres were finally sieved and sorted along their diameters in order to obtain a narrow size distribution. In this work, we focused on microspheres sorted between the sieves with nominal sizes 38 and 40 μm.

The TiO₂ microspheres were mixed with polyethylene powder and a pressure of 14 MPa was used to prepare rigid pellets with random spatial distribution of the TiO₂ microspheres. We observed that higher pressures (28 MPa) damage the TiO₂ microspheres. Pellets with thicknesses 1 and 3 mm were prepared. The concentration of rutile in the polyethylene matrix is determined by a precise measurement of the weight of the components. Taking into account the porosity the

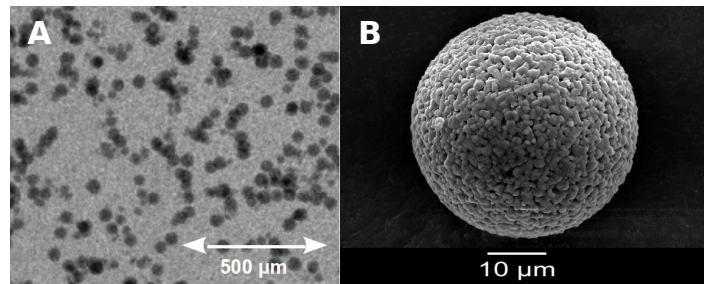


Fig. 1. TiO₂ microresonators (A) X-ray radiography of TiO₂ microparticles embedded in a polyethylene pellet (B) Scanning-electron-microscope image of the TiO₂ microparticle.

permittivity of rutile particles was about 92 [13]. For reference purposes, pure polyethylene pellets were prepared too. Using time-domain THz spectroscopy we found that such pellets exhibit a constant permittivity ($\epsilon_H = 1.98$) and negligible losses ($\tan \delta \sim 0.002$ around 1 THz).

3. Electromagnetic simulations

Dispersed dielectric microspheres with high permittivity represent a Mie resonance-based metamaterial, where the effective response relies on the resonance of individual elements while the coupling between isolated microparticles has only minor influence on the resonance properties. This allows us to simplify the theoretical investigations: we consider a periodic array of the microspheres and neglect the influence of the disorder. Note that this metamaterial behavior fundamentally differs from that of photonic crystals where the optical response is controlled mainly by the coupling between the constituents [14].

We employed a finite-difference time-domain (FDTD) simulation software package MEEP [15] to calculate the transmission and reflection spectra of TiO₂ microspheres with diameter $d = 35 \mu\text{m}$ arranged in a square lattice $a \times a$ and embedded in the centre of a slab with dielectric permittivity ϵ_H and thickness a . The filling fraction of TiO₂ in such a sample is $s = \pi d^3 / (6a^3)$. In order to account for the losses, the permittivity of rutile was considered as $92 + 2if$, where f is a frequency in THz [13]. The Nicolson-Ross-Weir (NRW) method [16–18] was used to retrieve the effective dielectric permittivity ϵ and effective magnetic permeability μ from the simulated spectra of the metamaterial.

We investigated how the filling fraction and the ratio between the permittivity of the microspheres and the host matrix affect the position and the strength of the magnetic response associated with the first Mie mode (Fig. 2). This resonance is located around 0.9 THz and its position changes only weakly in the studied range of the parameters. In Fig. 2(a) we observe that for $\epsilon_H = 2$ the permeability becomes negative for filling fractions $s > 5\%$. However, the strength of the resonance and the minimum negative value of the effective permeability decrease with increasing ϵ_H , as shown in Figs. 2(b, c). For $s = 18\%$, the range of the negative effective permeability completely disappears for the host material permittivity exceeding ~ 5 .

Attention must be paid to the conditions under which the structure can be approximated as homogeneous and described by effective parameters. For the host permittivity ϵ_H exceeding 3, the spectra of effective permeability μ start to strongly deviate from the resonance curve characteristic for a damped harmonic oscillator. Simultaneously, a pronounced antiresonance pattern emerges in the spectrum of effective permittivity [19]. These are signatures that the homogenization procedure is no more applicable when the lattice constant approaches the radiation wavelength in the host medium. A more general formalism is then required [20] describing the medium by effective permittivity $\epsilon(f, \vec{k})$ with explicit dependence on the wavevector \vec{k} .

The simulations demonstrate the existence and magnetic character of the first Mie resonance

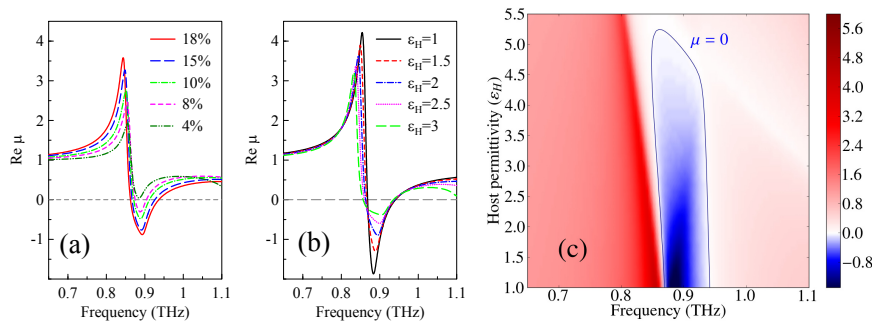


Fig. 2. Calculated effective magnetic permeability spectra $\mu(\omega)$ of a single layer of TiO_2 microspheres with diameter $35 \mu\text{m}$ arranged in a square lattice with unit cell $a \times a$ embedded in a medium with permittivity ϵ_H and thickness a . (a) Variable filling fraction s (and lattice constant a), host permittivity $\epsilon_H = 2$; (b,c) Variable host permittivity, $a = 50 \mu\text{m}$ (=filling factor of 18%). The colour scale in (c) represents the value of μ .

in our system near 0.9 THz and they show the possibility to achieve the negative permeability for filling fractions higher than 5% of rutile microspheres embedded in polyethylene.

4. Experiment

Time-domain THz experiments were performed using a custom-made setup described in [21] and a commercial Teraview THz spectrometer. Simultaneous determination of complex dielectric permittivity ϵ and complex magnetic permeability μ from spectroscopic measurements requires the acquisition of two independent complex quantities. In time-domain THz spectroscopy, the temporal profile of ultrashort THz pulses is measured, therefore multiple internal reflections of the THz beam in the sample appear as a series of mutually delayed echoes. For sufficiently thick samples, one can apply temporal windowing [22] and experimentally determine the transmittance T_m corresponding to the echo leaving the sample after $2m$ internal reflections (T_0 is the transmittance corresponding to a direct pass without internal Fabry-Pérot reflections). Such an approach enables various strategies for the retrieval of ϵ and μ . Here we employ the method where ϵ and μ are calculated from the transmittances T_0 and T_1 corresponding to the direct pass and to the first echo (Fabry-Perot reflection) in the sample, respectively [23]. Ref. [23] discusses also the experimental errors of evaluation of ϵ and μ , which are quite high due to the inherently lower accuracy in the experimental determination of the wave impedance.

5. Results

An example of effective magnetic permeability retrieved from T_0 and T_1 of a 3-mm thick pellet is shown in Fig. 3. A magnetic resonance around 0.9 THz is clearly resolved: this experimentally confirms the effective magnetic behavior of the metamaterial associated with this first Mie mode. Since all constituents are non-magnetic, the permeability at low frequencies should be equal to 1, in agreement with the observations. The slight tilt observed in $\text{Im } \mu$ is due to a minor phase shift caused by a long-term drift of the spectrometer. There is a very small contrast between refractive indices of the metamaterial and air, which leads to a weak Fresnel reflection, and consequently, to a weak first echo and transmittance T_1 (inset in Fig. 3). Small artefacts in the waveform of the order of $T_0/250$ may then cause the noise observed in the spectrum. In this situation, even a small crosstalk between signals belonging to T_0 and T_1 may cause a large error in the calculated transmission function T_1 . This crosstalk may really occur because the sharpness of the first Mie resonance leads to a long lasting ringing in the time-domain waveforms.

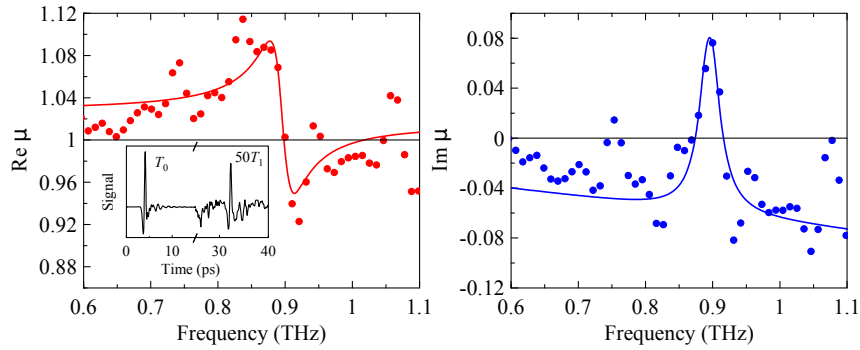


Fig. 3. Effective permeability of a 3 mm thick polyethylene pellet with low concentration ($\approx 0.15\%$) of TiO_2 around the first Mie resonance. Inset in the upper panel shows the waveform of raw experimental data. The signal corresponding to the first internal reflection is multiplied by 50 to make it visible.

The resonance in Fig. 3 was fitted using the damped harmonic oscillator model, which leads to a central frequency of 0.896 THz and a damping of 41 GHz. The direct pass T_0 and the first echo T_1 are detected with a time delay of 28 ps which limits the time window for the Fourier analysis to $\Delta t \approx 26$ ps. This determines the frequency resolution of the experiment (~ 38 GHz) and, consequently, it broadens the measured width of the resonance [11]; the deconvoluted width of the first Mie mode is then 15 ± 5 GHz. Such a damping is much smaller than that observed in a dense monolayer of these microparticles reported in [13]. The microspheres in the pellets are much sparser: the weaker damping may indicate that the coupling between individual microspheres is reduced. Since, namely in the vicinity of the resonance, T_1 rapidly decreases with increasing filling factor, the retrieval of ϵ and μ from T_0 and T_1 fails for filling factors exceeding tenths of percent. For this reason, we carried out the investigations with higher filling factor based solely on the transmittance amplitude obtained from long time-domain scans which involved the sum of all measurable Fabry-Pérot reflections (Fig. 4).

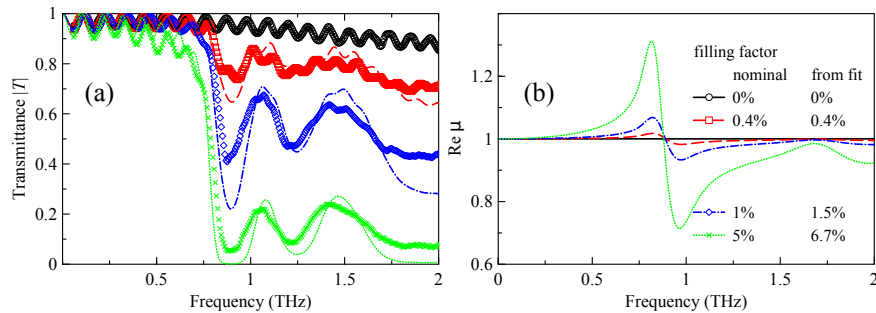


Fig. 4. (a) Transmission spectra of 1 mm-thick polyethylene pellets with various concentrations of TiO_2 spheres. Symbols: experimental data, lines: fits using Maxwell-Garnett theory. (b) Effective permeability corresponding to the fitted transmission spectra. Filling factors were obtained from the component weights (nominal values) and from the fits.

In order to gain further insight into the properties of the metamaterial, we employed a dynamic Maxwell-Garnett theory [24], in which we account for the distribution of sizes of the microspheres. It turns out that a size distribution with two characteristic mean radii r_1 and r_2

needs to be considered to reproduce the observed transmittance spectrum:

$$g(r) = \frac{w}{\sqrt{2\pi}\sigma} \exp\left[-\frac{(r-r_1)^2}{2\sigma^2}\right] + \frac{1-w}{\sqrt{2\pi}\sigma} \exp\left[-\frac{(r-r_2)^2}{2\sigma^2}\right], \quad (1)$$

where σ is the width of the distributions, and w and $1-w$ are the weights of the first and second size, respectively. We denote by c_{tot} the total number of spheres per unit volume; then $c_{tot}g(r)dr$ is the number density of spheres with the size in the range $(r, r+dr)$. The effective permittivity ε of a composite containing such a distribution of spheres with the polarizabilities $\alpha(r)$ reads:

$$\frac{\varepsilon - \varepsilon_H}{\varepsilon + 2\varepsilon_H} = \frac{1}{3\varepsilon_0\varepsilon_H} \int_0^\infty c_{tot}g(r)\alpha(r)dr. \quad (2)$$

The polarizability $\alpha(r)$ is obtained from the Mie theory [24, 25] as $\alpha(r) = 4\pi\varepsilon_0\varepsilon_H 3ia_1(r)/(2k^3)$, where $k = 2\pi f\sqrt{\varepsilon_H}/c$ is the wave vector of radiation in the host medium and a_1 is the electric-dipole Mie coefficient of a sphere with radius r . Similar equations can be derived also for the magnetic response where the magnetic-dipole Mie coefficient b_1 is introduced. We finally find:

$$\varepsilon = \varepsilon_H \frac{k^3 + 4\pi ic_{tot} \int_0^\infty g(r)a_1(r)dr}{k^3 - 2\pi ic_{tot} \int_0^\infty g(r)a_1(r)dr} \quad \mu = \frac{k^3 + 4\pi ic_{tot} \int_0^\infty g(r)b_1(r)dr}{k^3 - 2\pi ic_{tot} \int_0^\infty g(r)b_1(r)dr}. \quad (3)$$

The use of the Maxwell-Garnett theory is well justified, because the concentration of microspheres is low (below 5%) and the spatial distribution is random. In the fits the transmission T was calculated using the standard Airy formula including all internal reflections.

A good match between the calculated and measured spectra is found for mean particle radii $r_1 = 17 \mu\text{m}$, $r_2 = 13.5 \mu\text{m}$ and a distribution width $\sigma = 1 \mu\text{m}$. These parameters are supported by a optical microscope analysis, which revealed a comparable ellipticity of the microparticles. Furthermore, the filling factors obtained from the fit by the Maxwell-Garnett theory (0.4%, 1.5% and 6.7%) are in good agreement with those determined from the weights of the components when preparing the pellets (0.4%, 1.0% and 5%, respectively). Note that in the Maxwell-Garnett theory calculations, we optimized the thickness of the pellets (typically within 30 μm) in order to match the interference pattern at low frequencies.

6. Conclusion

We fabricated rigid metamaterials made of TiO_2 spherical microresonators embedded in polyethylene. We observed a magnetic effective response in the vicinity of the first Mie resonance. Using finite-difference time-domain calculations of the effective response we found that a range of negative effective magnetic permeability can be achieved for sufficiently high filling factors and contrasts between the permittivities of the resonators and the embedding medium. The developed structures are prototypes of cheap mechanically stable terahertz metamaterials.

Funding

LabEx AMADEus (ANR-10-LABX-42); the Czech Science Foundation (14-25639S).

Acknowledgments

MŠ is grateful to Ashod Aradian for stimulating discussion about the Maxwell-Garnett theory.